Materials Research Proceedings 41 (2024) 2514-2523 https://doi.org/10.21741/9781644903131-277

Perforation resistance of some materials in 3D printed parts

NICOLAU Mihaela[1,a], HRITUC Adelina[1,b *], MIHALACHE Marius-Andrei[1,c], NAGÎT Gheorghe[1,d], DUȘA Petru[1,e], CRĂCIUN Elisaveta[1,f], MUNTEANU Adriana[1,g], DODUN Oana[1,h], SLATINEANU Laurențiu[1,i]

[1]Gheorghe Asachi" Technical University of Iaşi, Department of Machine Manufacturing Technology, Blvd. D. Mangeron, 39 A, 700050 Iaşi, Romania

[a]mihaela.nicolau@student.tuiasi.ro, [b]adelina.hrituc@student.tuiasi.ro, [c]andrei.mihalache@tuiasi.ro, [d]nagit@tcm.tuiasi.ro, [e]pdusa@tcm.tuiasi.ro, [f]elisaveta.craciun@student.tuiasi.ro, [g]adriana.munteanu@academic.tuiasi.ro, [h]oanad@tcm.tuiasi.ro, [i]slati@tcm.tuiasi.ro

Keywords: Perforation Resistance, Testing Equipment, 3D Printing, Finite Element Modeling, Experimental Test Empirical Mathematical Model

Abstract. Sometimes, for various reasons, some parts manufactured by 3D printing need to have high perforation resistance. In such situations, it is necessary to know the perforation resistance values of the materials incorporated in the parts. In principle, conical tip penetrators are allowed to fall under their weight on the test sample material to be investigated, which allows the conical tip to penetrate and advance into the sample material. A finite element modeling allowed obtaining some information about the behavior of the material during the perforation action. Perforation resistance testing equipment has been designed to use conical tips and different heights from which the penetrator is released. Thus, it became possible to highlight the influence of some input factors in the testing process on the diameter of the hole generated by the penetrator in the thermoplastic polyurethane-type material of the test sample. As input factors, the weight of the penetrator, the drop height of the penetrator, and the thickness of the test sample were considered. The mathematical processing of the experimental results allowed the establishment of some empirical mathematical models, which highlight the influence exerted by the three input factors on the value of the considered output parameter. It was confirmed that as the penetrator weight and drop height increase, the diameter of the hole generated in the sample material increases. In contrast, the test sample thickness exerts the opposite effect.

Introduction

In 2009, ASTM defined additive manufacturing (AM) as "a process of joining materials to make objects from 3D model data, usually layer upon layer, as opposed to subtractive manufacturing methodologies" [1,2]. Since its inception, additive manufacturing has been widely used in many applications in different industries and research fields due to the many benefits it brings in manufacturing, design, and distribution, such as freedom of design, flexibility, customization, waste minimization, and sustainability of production in the artistic, medical, marketing, and educational fields [3-6].

Fused deposition modeling (FDM) is an additive manufacturing process in which a thin filament of plastic (thermoplastic polymer) is melted and extruded (dispensed through a nozzle) in a thickness typically of 0.25 mm [5]. Due to the properties of the materials used in the process, FDM can generate rigid and flexible parts. Materials used in this process are PLA (polylactic acid), PC (polycarbonate), PET (polyethylene terephthalate), TPU (thermoplastic polyurethane) (flexible), ABS (acrylonitrile butadiene styrene), polyphenylsulfone, and nylon 6 [7].

Typical applications include the production of parts and functional prototypes with outstanding thermal and chemical resistance and excellent strength-to-weight ratios, such as jigs, fixtures,

turbines, rotors, bumpers, and more [8]. According to Melnikova *et al.* (2014), ABS is too brittle for textile industry applications, but a soft version of PLA can be used to manufacture textile-based structures. In this case, the hard PLA is polylactic acid with some useful properties (elongation at break ~ 4 %, tensile modulus 1968 MPa), while a soft PLA is PLA including a softener (with elongation at break up to ~ 200 %) [9].

In the textile area, AM is used to manufacture textiles, flexible structures, and flexible materials, resulting in structural materials frequently used, for example, in the medical field [10].

Any manufactured part is usually tested to confirm that the intended design was achieved. Conventional tests such as tensile, flexure, Poisson's ration, axial fatigue, and compression tests [11] can be supplemented by any non-destructive tests, such as hardness tests, that do not directly measure a mechanical characteristic [12]. Due to the possibility of obtaining an uneven-density product through the FDM process, an indentation test applies an uneven stress distribution on the sample to predict the mechanical behavior of materials [13].

In the indentation test, the stress experienced by the material is due to both elastic and plastic deformation. In the beginning, elastic deformation is predominant until a certain depth is reached, after which plastic deformation localizes around the indenter edge and then expands along with indentation depth. The test output is usually the indentation depth or the size of the imprint, which correlates the material hardness to indenter geometry and indentation parameters [14]. Low-load indentation techniques have been developed for testing metallic and ceramic thin films or coatings, requiring several tests and statistical data treatment [14]. According to Riccardi at al. (2004), a flat-end punch with a diameter of 1 mm or smaller and axial length equal to 1.5 mm was used on a massive frame, dimensioned to have a total elastic deformation of about 1 μm so that elastic modulus and yield stress can be directly determined from pressure-penetration curves by applying simple analytical relationships.

According to Alisafaei et al. [13], many studies have been done using a sharp Berkovich tip and show the numerous variables that can affect the results. Lambiase et al. (2023) [12] show that the tests using a sharp tip are heavily influenced by the density of the material being tested, which in turn is defined by the thickness of the sample. In [15], the authors investigate the perforation resistance of glass fiber-reinforced polyetherketoneketone (PEKK) composites. The study focuses on evaluating the composite material's ability to withstand perforation and provides insights into its mechanical properties. The findings contribute to the understanding of the performance of glass fiber-reinforced PEKK composites, offering valuable information for applications requiring high resistance to perforation. The impact resistance and compression behavior of carbon fiber-reinforced polyetheretherketone (CF/PEEK) laminates are experimentally investigated after hot-press fusion repair, considering various stacking sequences [16]. The results emphasize the performance of repaired laminates under impact and compression and offer relevant information for the development and maintenance of composite structures. According to Popa et al. [17], the AM materials can be numerically modeled and calibrated with the experimental ones.

For textile additive manufacturing, the adhesion of the printed material onto the chosen apparel is a serious issue [18], and it is being managed through adhesion tests, known as mechanical peel tests [19 -21]. Other tests include tear strength, bending length measurements, abrasion testing, wetting and cyclic bending, and the effect of washing [18].

The International Standards Organization (ISO) proposed a standard (ISO 17296-3:2014 Additive Manufacturing – General Principles—Part 3: Main characteristics and corresponding test methods [19]) to address the quality characteristics of parts produced by AM [22].

According to Maidin et al. [23], a stab test was performed on an AM material (PC-ABS) of various thicknesses, from 4.0 to 10.0 mm, using an impact energy of 24 joules to determine a minimum thickness that resulted in a maximum penetration of 7.0 mm by using Instron CEAST

9340 Drop Impact Tower. The results demonstrated that the thickness must be at least 8.0 mm for the desired results.

The research, the results of which are presented in this paper, aimed to initiate some investigations regarding the resistance to perforation of test samples made of a polymer. The analysis of the conditions in which the perforation resistance can be experimentally tested showed that it is possible to use a dynamic test based on the impact produced by the fall from a certain height of a penetrator with the material of the test sample. Adequate equipment was designed to allow the fulfillment of the specific conditions of the proposed material. Later, through the mathematical processing of the experimental results, empirical mathematical models were identified to highlight the influence of the input factors considered on the diameter size of the hole generated by the penetrator in the sample material.

Premises for testing the perforation resistance of parts manufactured by 3D printing

For testing the resistance of the material of parts manufactured by 3D printing, it could use test schemes involving a dynamic effect (fast penetration of a penetrator into the material of the part) and quasi-static ones, where there is a slow penetration or in successive stages of the penetrator in the material of the part.

In the case of the present investigation, a dynamic test scheme was adopted based on the fall under the action of the weight of a cone-shaped penetrator from a determined height. Such a way of testing perforation resistance requires the existence of appropriate equipment. As a parameter to evaluate the perforation resistance, the diameter of the hole generated in the test sample material by the penetrator or the penetration depth of the penetrator in the part material could be considered (Fig. 1). It is expected that for perforation-resistant materials, the diameter of the hole generated by the penetrator or the penetration depth will be smaller.

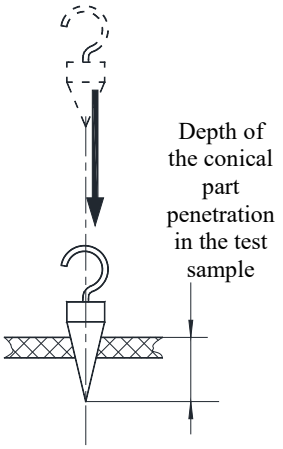

Fig. 1. Scheme of testing a material from the point of view of resistance to perforation

The main factors that affect the value of the output parameter specific to the perforation test under the mentioned conditions are the shape and weight of the penetrator, the height from which the penetrator falls, and some physical and mechanical properties of the material of the tested part. It is known that such physical-mechanical properties of the material of a part manufactured by 3D printing depend on the material's nature and the material's internal structure. The last factor taken into account (the physical structure of the part material) can be decisively influenced by the values of the factors that characterize the 3D printing conditions (thickness of the deposited layer, the percentage infill, the infill pattern, the type of printing network, the printing temperature, the cooling conditions, etc.).

Experimental conditions

The experimental research aimed to identify some possibilities of highlighting the influence exerted by several input factors in the perforation process on an output parameter of this process. The diameter of the hole made by the penetrator in the test samples was chosen as such output parameter. The experimental tests were carried out using the equipment schematically represented in Fig. 2. This equipment was designed to be usable on a drilling machine. A cone-shaped penetrator (Fig. 3) was allowed to fall freely from a certain height. The release of the

Materials Research Proceedings 41 (2024) 2514-2523 https://doi.org/10.21741/9781644903131-277

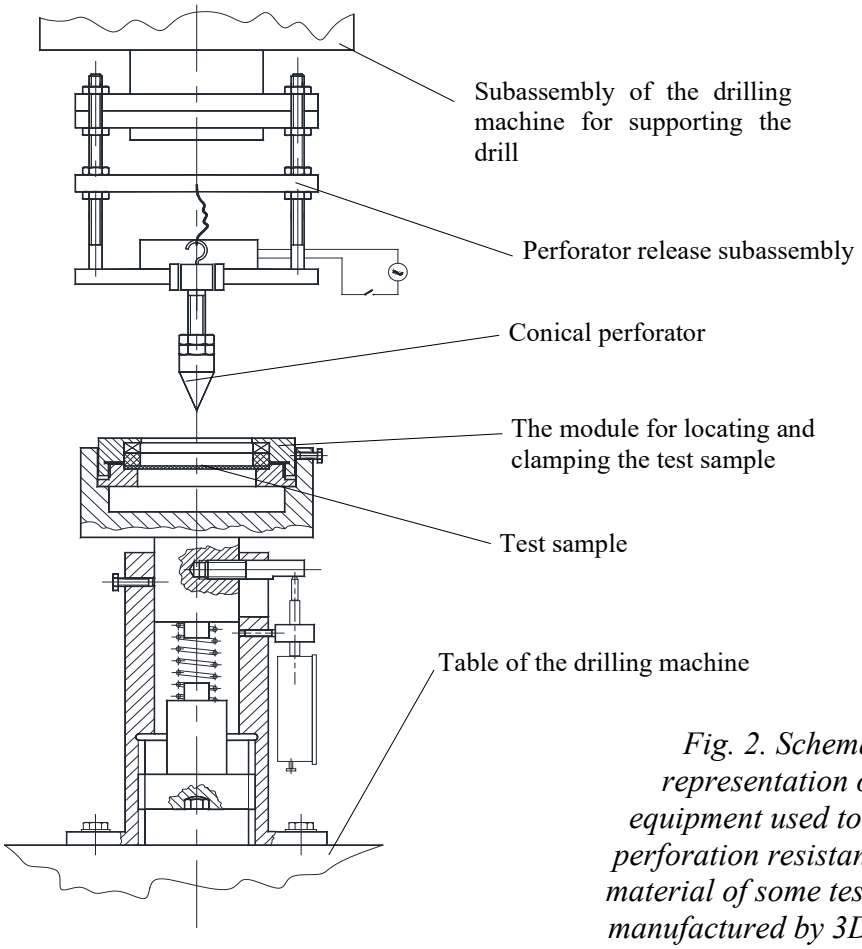

Fig. 2. Schematic representation of the equipment used to test the perforation resistance of the material of some test samples manufactured by 3D printing

penetrator was carried out by means of a sub-assembly with an electromagnet mounted on the flange of the bushing in which the main shaft of the drilling machine rotates.

The material from which the samples were made was thermoplastic polyurethane (test samples with a diameter of 45 mm and with different thicknesses). The samples were manufactured by 3D printing on an Ultimaker 3 printer (Netherlands). The 3D geometries design included the corresponding samples' 0.4 mm and 0.8 mm thickness values. Due to the particular nature of the flexible filament produced by FormFutura, the 3D printer produced samples of 0.56 mm and 0.94 mm in thickness when using *.stl* files. Values are higher because of the complexity of the geometry, which contains an array of square holes of 1.5 mm, which forces the extruder to its maximum. The main printing conditions were the following: printing speed v=20mm/s, layer thickness l = 0.1mm, infill density i= 100%, zig-zag infill pattern.

The 3D model was imported as a .stl file in the Ultimate Cura version 5.5.0 software. It was decided upon a fine printing profile that uses 0.1 mm of layer height. The wall line count was set to three with the same value as the layer height for the outer wall wipe distance. Wall ordering was set from outside to inside for better dimensional accuracy. The seam alignment on the Z axis was user-specified so it could allow a back-right position. The top and bottom layers were left with default settings, but the infill density was set to 100% so it would not affect the integrity of samples by using different values and patterns. Because of the number of travels and retractions that have to be made and the special flexible nature of the filament, the infill speed was set to 20 mm/s.

The printing process, the Fused Deposition Modelling (FDM), produced unexpectedly higher dimensional values than the ones from CAD design. Results and observations about this phenomenon are going to be detailed in a future scientific paper. The 3D Python Flex 90A filament

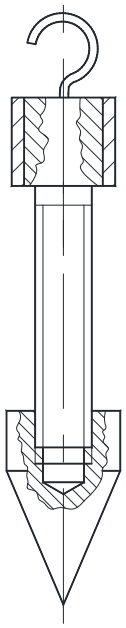

Fig. 3. The penetrator used for testing the perforation resistance of the material of some specimens manufactured by 3D printing

produced by FormFutura has a shore hardness of 90A, can elongate up to 500%, has a tensile strength of 35 MPa, and a tear strength of 90 N/mm^2. Prints were carried out with respect to the manufacturer's recommendations. Each set of samples included two additional test samples for validation purposes.

Each test sample was rigidly fixed in a support module located, in turn, in a sub-assembly mounted on the table of the drilling machine (Fig. 2). When designing equipment, a solution was also taken into account to allow the evaluation of the impact force. For this purpose, a sub-system with a spring was included in the sub-assembly located on the drilling machine table. The compression of the spring under the action of the impact force can be highlighted using a dial gauge. When it is not intended to evaluate the magnitude of the impact force, spring compression no longer occurs due to the use of a locking screw. The possibility of changing the weight of the penetrator (Fig. 3) has been provided by mounting one or more nuts on the central rod.

Releasing the penetrator causes it to move toward the test sample and make a hole. When the impact force is higher, due to the increase in the height *h* from which the penetrator falls or the increase in the mass of the penetrator, the hole made in the test sample has a larger diameter. The diameter of the hole was determined using an optical microscope type ISM-PM600SA, with magnification 10x-200x, short focus distance, resolution 1600x1200, and software corresponding to this microscope (ISM-PRO). An image of a hole obtained with the help of a digital microscope is shown in Fig. 4. Due to a certain fragility of the sample material, some holes did not have a circular shape but were closer to that of an irregular polygon with partially curved sides. In such situations, the diameter of the irregular polygon's circumscribed circle was considered.

Finite element modeling of the phenomena that develop during the puncture resistance testing process

It was intended to model, using the finite element method (FEM), the response of a polymeric circular sample to a solicitation imposed by a perforating element. Experimental tests revealed that different deformations were recorded depending on the parameters used for 3D printing of samples, which, in visual terms, show irregulated shaped holes. By measuring hole dimensions, time-of-travel of the penetrator, and other parameters, it can establish relationships between solicitation and the response it produces. However, perforation generates stress and strain, which can be very difficult to assess by traditional methods. By simulating the same environment, it aims to achieve the same type of responses as the ones produced during experimental tests. That would allow us to evaluate stress and strain distribution numerically.

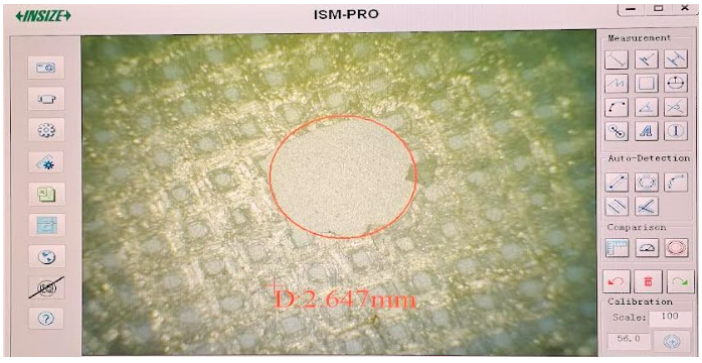

Fig. 4. Optical microscope image of a hole made by punching the 3D printed polymer sample

Ansys (researcher license) was the preferred software choice for FEM analysis. It used TPU type of material retrieved from TotalMateria database. Explicit dynamics allow large deformation

and were the choice for the simulation module. The 3D geometry was modeled inside SolidEdge (Teacher edition) concerning the dimensions of parts used in experimental tests. The penetrator and the ring on which the circular sample sits were assigned structural steel material, whereas the test sample with a thickness of 0.56 mm received the TPU. The setup includes default body interactions and a single bonded contact between the upper facet of the support ring and the polymeric sample's lower facet, which was assigned with an asymmetric behavior.

Mesh-wise, element order was set to linear. Because perforation appears near the center of the sample, it was needed a finer mesh in that area for FEM to capture appropriate results. The solution was a new user-defined coordinate system assigned to a node that was the penetrator's tip. Two body sizing methods based on the sphere of influence for the penetrator and the circular sample were used. Element size was set to 1 mm and 4 mm for the sphere's radius. It used a hex dominant method, which involves hexagons as the preferred type of finite element for the 3D sample. This produced 4013 nodes and 5048 elements, which are tetrahedral elements with 4 nodes (Tet4), hexahedron elements with 8 nodes (Hex8), wedge (prism) elements with 6 nodes (Wed6) and pyramidal elements with 5 nodes (Pyr5).

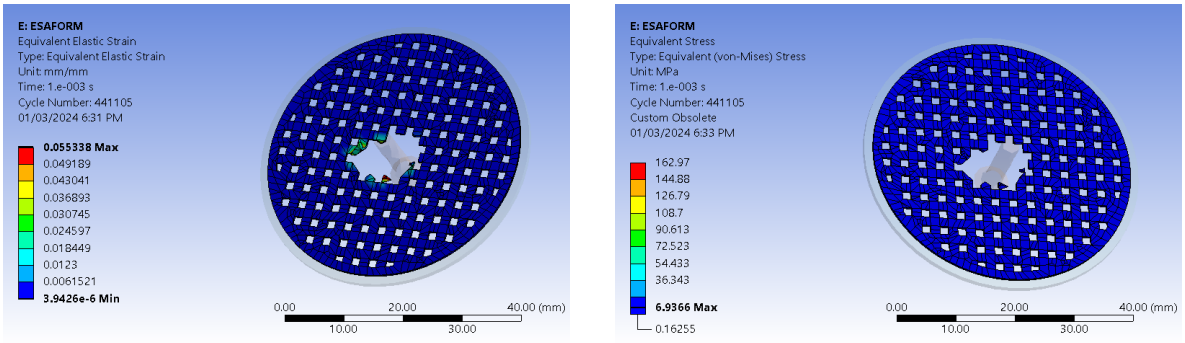

a) b)

Fig. 5. Graphical representations of FEM results: a) distribution of equivalent elastic stress; distribution of equivalent (von-Mises) stress.

Conditions include a displacement value of −4 mm on *Z* axis for the penetrator and a fixed support assigned to the lower facet of the support ring. Analysis settings considered 0.001 s end time with explicit time integration for one load step. Erosion controls allow the solver to continue when the geometric strain limit of 100% is being achieved. Results are visual consistent with the ones retrieved from experimental tests. Equivalent elastic strain (see Fig. 5.a) peaks at 0.55338 mm/mm, whereas the equivalent stress evaluated according to von Mises criteria registers a maximum value of 162.97 MPa (see Fig. 5.b). Comparisons between the results of FEM and experimental tests are not included in the present paper as they are subjected to those mentioned above in future scientific papers. The aim of using FEM in the present paper was to highlight the distribution of stress and strain after the tensile strength of the material is overpassed and the perforation occurs within the area of interest. Deformation-wise, one may observe that the thickness of the material is slightly overpassed when the perforation occurs at high speed, thus not giving the material time to elongate as it should, according to the producer's technical data sheet. The presented results were obtained with significant use of computing power. The authors acknowledge that refinement of the results may be needed and recommend that they should be used with care.

Experimental results

The input factors in the perforation process were the weight *w* of the penetrator, the distance *h* between the tip of the penetrator and the test sample, and the thickness *t* of the test sample, respectively. It was appreciated to carry out the experimental tests in accordance with the

requirements of a full factorial experiment, with 3 independent variables at 2 levels of variation [24, 25]. Therefore, two values of the weight w of the penetrator were used (w_{min}=45·10^{-2} N, w_{max}=75·10^{-2} N), of the distance h between the penetrator and the test sample (h_{min}=140 mm, h_{max}=280 mm) and of the thickness t of the test sample (t_{min}=0.56 mm and t_{max}=0.94 mm).

Table 1. Conditions and results of experimental tests.

Exp. No.	Input factors			Diameters of the holes made for three measurements [mm]			The average diameter of the holes made in the test sample, d [mm]
	Weight, w [g]	Height, h [mm]	Thickness, t [mm]	1	2	3	
1	45	140	0.56	2.647	2.596	2.624	2.62
2	45	140	0.94	0.735	0.769	0.791	0.76
3	45	280	0.56	2.675	2.715	2.631	2.67
4	45	280	0.94	1.405	1.277	1.285	1.32
5	75	140	0.56	5.107	4.983	5.05	5.05
6	75	140	0.94	1.979	1.945	1.918	1.95
7	75	280	0.56	5.509	5.435	5.455	5.47
8	75	280	0.94	3.118	3.08	3.101	3.10

Some of the experimental conditions and the obtained results are listed in Table 1. A single experimental trial was performed for each set of conditions considered.

Processing of experimental results

The experimental results were mathematically processed using specialized software [25]. The aim was to determine an empirical mathematical model that highlights the influence exerted by the three input factors in the testing process (the weight w of the penetrator, the height h from which the penetrator is released, and the thickness t of the test sample) on the value of the diameter d of the hole generated by the penetration of the penetrator into the test sample material.

Said software provides conditions for selecting the most appropriate mathematical model from five predefined models (first-degree polynomial, second-degree polynomial, power-type function, exponential function, hyperbolic function). The selection of the most appropriate model among the five possible models is performed using Gauss's criterion [25, 26]. The lower the value of Gauss's criterion, the more appropriate the mathematical model can be considered in relation to the experimental results used to determine it. By using the specialized software, it was found that the most appropriate mathematical model is a polynomial of the first degree:

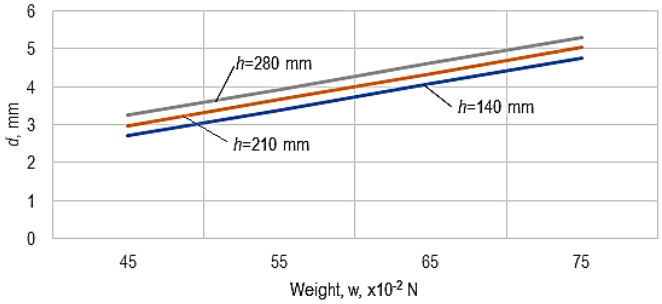

Fig. 6. The influence of the size of the weight w on the diameter size d of the hole in the test sample for different values of the height h (t = 0.55 mm)

$$d = 2.232 + 0.0683w + 0.00389h - 5.71t, \quad (1)$$

the value of Gauss' criterion being, in this case, S_G=0.1586501.

Since power-type functions are commonly used in manufacturing, a mathematical model of this type was also determined:

$$d = 0.000309w^{1.551}h^{0.401}t^{-1.670}, \quad (2)$$

for which the value of Gauss's criterion is S_G=0.219436. In the case of the power function type mathematical model, the value of Gauss's criterion is higher than that of the first-degree polynomial. Still, the power type function allows for the acquisition of direct information regarding the intensity of the influence exerted by the input factors on the value output parameter *d*.

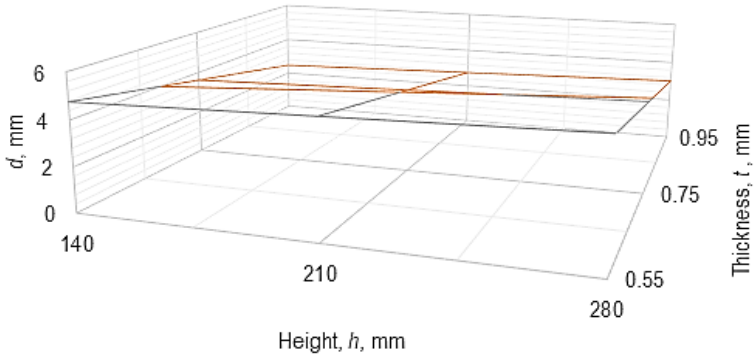

Fig. 7. The influence of the height h and the thickness t of the test sample on the diameter size d of the hole in the test sample (w=75·10^{-2} N)

The graphical representations in Figs. 6 and 7 were made by using the mathematical model of the first-degree polynomial type. The analysis of these graphical representations and the mathematical models constituted by equations (1) and (2) shows that, as expected, the diameter *d* of the hole in the test sample increases when the weight *w* and height *h* values increase. This fact can be explained by increasing the kinetic energy when the penetrator hits the test sample material. An increase in the thickness *t* of the test sample leads to a decrease in the diameter *d* of the hole due to the absorption by the thicker material of the test sample of a greater amount of the kinetic energy corresponding to the impact between the penetrator and the material of the test sample. It is also found that the strongest influence on the increase in the value of the diameter *d* is exerted by the weight *w*, which is associated with higher values of the coefficient (in Eq. (1)) and, respectively, of the exponent (in Eq. (2)). A more suggestive illustration of the intensity of the effects exerted by the three considered input factors is possible by developing a graphic representation of the average responses of the investigated process to the values of the input factors at two levels (Fig. 8).

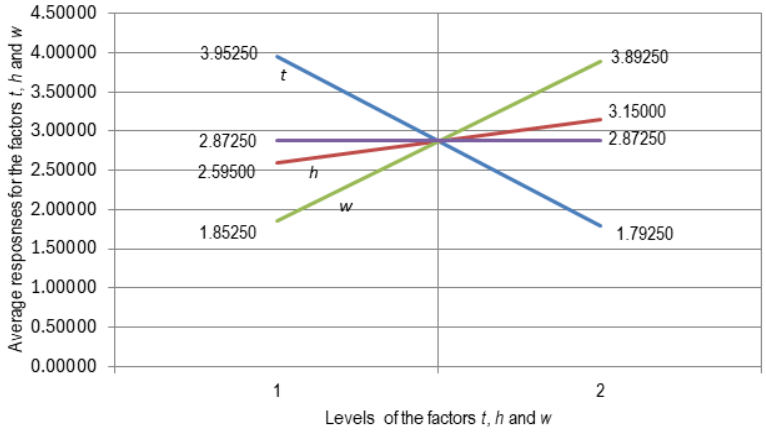

Fig. 8. Mean response values for the two levels of input factor variation

The average responses were determined as averages of the values of the output parameters corresponding to the placement on the same level of the values of the input factors [24].

Analysis of the graphical representation in Fig. 8 confirms that increasing the values of weight *w* and height *h* will increase the value of diameter *d*, while increasing the thickness *t* of the test sample will decrease the value of diameter *d*. In this case, the intensity of the input factors' influence on the output parameter's value is evidenced by the slope of the line segment corresponding to a certain input factor.

Conclusions

The resistance to perforation of a material means the resistance that that material opposes to the penetration of a penetrator having a certain shape. The study of specialized literature related to the

perforation resistance of some materials in the composition of parts manufactured by 3D printing highlighted that, for various reasons, such a problem is a concern of researchers in the field of additive manufacturing. The research, the results of which are presented in this paper, aimed to obtain information regarding the perforation behavior of small-thickness samples made of thermoplastic polyurethane. A finite element modeling was used to identify some aspects of interest in relation to the processes that develop in the perforation zone. A perforation test equipment adapted to a drilling machine was designed to highlight the influence of various factors on the perforation resistance of disc-shaped test samples. As input factors, the size of the penetrator weight, the height from which the penetrator is released, and the thickness of the test sample were considered. The diameter of the hole generated in the test sample by releasing the penetrator from a certain height was measured. Through the mathematical processing of the experimental results, it was found that the factor with the greatest influence on the perforation resistance is the weight of the penetrator. Empirical mathematical models of the first-degree polynomial-type and power-type functions allowed to highlight the intensity of the influence exerted by the input factors on the resistance to perforation. It is intended to continue the research in the future by also taking into account the influence exerted by the 3D printing parameters on some sizes that characterize the resistance to perforation.

References

[1] T. Sprinkle, The 5 most important standards in additive manufacturing. Information on https://sn.astm.org/features/5-most-important-standards-additive-manufacturing-.html#:~:text=Although%20it%20has%20since%20been,is%20still%20in%20use%20today.

[2] J. Alcisto, A. Enriquez, H. Garcia, S. Hinkson, T. Steelman, E. Silverman, P. Valdovino, H. Gigerenzer, J. Foyos, J. Ogren, J. Dorey, K. Karg, T. McDonald, O.S. Es-Said, Tensile Properties and Microstructures of Laser-Formed Ti-6Al-4V, J. Mater. Eng. Perf. 20 (2011) 203–212. https://doi.org/10.1007/s11665-010-9670-9

[3] M. Mehrpouya, A. Vosooghnia, A. Dehghanghadikolaei, B. Fotovvati, The benefits of additive manufacturing for sustainable design and production, in: Sustainable Manufacturing. Elsevier, 2021, 29–59. https://doi.org/10.1016/B978-0-12-818115-7.00009-2

[4] P. P. Kruth, Material incress manufacturing by rapid prototyping techniques, CIRP Ann. Manuf. Tech., vol. 40, no. 2 (1991) 603–614. https://doi.org/10.1016/S0007-8506(07)61136-6

[5] K. V. Wong, A. Hernandez. A Review of Additive Manufacturing, ISRN Mechanical Engineering (2012) 208760. https://doi.org/10.5402/2012/208760

[6] Information on https://www.materialseducation.org/educators/matedu-modules/docs/Materials_in_FDM.pdf

[7] A.D. Mazurchevici, D. Nedelcu, R. Popa, Additive manufacturing of composite materials by FDM technology: A review, Indian J. of Eng. & Mater. Sc., 27 (2020) 179-192

[8] Information on https://www.stratasys.com/en/stratasysdirect/technologies/3d-printing/fused-deposition-modeling/

[9] R., Melnikova1, A., Ehrmann1, K., Finsterbusch, 3D printing of textile-based structures by Fused Deposition Modelling (FDM) with different polymer materials, *IOP Conf. Ser.: Mater. Sci. Eng.,* 62 (2014) 012018. https://doi.org/10.1088/1757-899X/62/1/012018

[10] D.B. Sitotaw, D. Ahrendt, Y. Kyosev, A.K. Kabish, Additive Manufacturing and Textiles—State-of-the-Art, Applied Sciences, 10, no. 15 (2020) 5033. https://doi.org/10.3390/app10155033

[11] Information on https://advanses.com/mechanical-testing-of-3d-printed-parts-and-materials/

[12] F. Lambiase, S.I. Scipioni, A. Paoletti, Mechanical characterization of FDM parts through instrumented flat indentation. Int. J. Adv. Manuf. Technol., 125, (2023) 4201-4211. 10.1007/s00170-023-10992-3

[13] F. Alisafaei, C-S. Han, Indentation depth dependent mechanical behavior in polymers. Adv. Condens. Matter. Phys. (2015) 1-20. https://doi.org/10.1155/2015/391579

[14] B. Riccardi, R. Montanari, Indentation of metals by a flat-ended cylindrical punch. Mater Sci Eng: A 381,(1–2) (2004) 281–291. https://doi.org/10.1016/j.msea.2004.04.041

[15] N.A. Nassir, R.S. Birch, W.J. Cantwell, Q.Y. Wang, LQ. Liu, Z.W. Guan, The perforation resistance of glass fiber reinforced PEKK composites. Polymer Testing 72 (2018) 423-431 https://doi.org/10.1016/j.polymertesting.2018.11.007

[16] A. Liu, Y. Zhou, Y. Chen, J., Hu, B. Wang, Experimental investigation of impact resistance and compression behavior of CF/PEEK laminates after hot-press fusion repair with different stacking sequences. Polymer Composites (2023) 1-15. https://doi.org/10.1002/pc.27571

[17] C.F. Popa, T. Krausz, S.V. Galatanu, Numerical and experimental study for FDM printed specimens from PLA under IZOD impact tests, Mater. Today Proc., 78, 2 (2023) 326-330. https://doi.org/10.1016/J.MATPR.2022.11.501

[18] E.M. Keefe, J. A. Thomas, G. A. Buller, C. E. Banks, Textile additive manufacturing: An overview, Cogent Engineering, 9:1 (2022) 1-17. https://doi.org/10.1080/23311916.2022.2048439

[19] Y. Zhang, Y., Liu, X., Ji, C.E., Banks, W., Zhang, Flower-like hydroxyapatite modified carbon paste electrodes applicable for highly sensitive detection of heavy metal ions. J. Mater. Chem., 21 (2011) 7552-7554. https://doi.org/10.1039/c1jm10949a

[20] Information on https://bura.brunel.ac.uk/bitstream/2438/18700/1/FullText.pdf

[21] G.H. Loh, A. Sotayo, E. Pei, Development and testing of material extrusion additive manufactured polymer–textile composites, Fash. Text. 8, 2 (2021). https://doi.org/10.1186/s40691-020-00232-7

[22] Information on https://nvlpubs.nist.gov/nistpubs/ir/2015/NIST.IR.8059.pdf

[23] S. Maidin, S. Ying Chong, T. Kung Heing, Z. Abdullah, R. Alkahari, Stab resistant analysis of body armour design features manufactured via fused deposition modelling process, in: F. Uddin (Ed), Textile Manufacturing Processes. IntechOpen, 2019. https://doi.org/10.5772/intechopen.86439.

[24] R. Ranjit, A primer on the Taguchi Method, 2nd edition, SME, 2010.

[25] G. Crețu, Fundamentals of experimental research. Laboratory handbook. “Gheorghe Asachi” Technical University of Iaşi, Iaşi, Romania, 1992 (in Romanian).

[26] A.G. Worthing, J. Geffner, Processing the experimental data. Technical Publishing House, Bucharest, Romania, 1959 (in Romanian).